 DOI: 10.1002/masy.201050520

Novel Routes to Functional (Meso)Porous Cross-Linked Polymers Using (Semi-)Interpenetrating Polymer Networks as Nanostructured Precursors

Daniel Grande,[*1] *Isabelle Beurroies,*[2] *Renaud Denoyel*[2]

Summary: Semi-interpenetrating polymer network (semi-IPN) and IPN systems based on poly(D,L-lactide) and a functional vinylic polymer can be effectively used as nanostructured precursors to novel functionalized (meso)porous networks. Indeed, the extraction of uncross-linked oligoesters from semi-IPNs as well as the quantitative hydrolysis of the polyester sub-network associated with semi-hydrolyzable IPNs constitute straightforward and versatile strategies for engineering (meso)porous cross-linked polymers with miscellaneous functionalities. The versatility of both complementary routes was illustrated through the generation of methacrylic porous networks with acidic (COOH, SO_3H) functions as well as styrenic porous networks with acidic (COOH, SO_3H) or basic (pyridine) functions. The potentialities afforded by the two approaches were discussed, and more particularly the porous networks derived therefrom were characterized by several physico-chemical techniques.

Keywords: aliphatic polyesters; extraction; hydrolysis; (meso)porous polymers; (semi-)interpenetrating polymer networks (IPNs)

Introduction

Over the last decades, much attention has been paid to the design of porous materials as they are involved in a wide range of applications, *e.g.* nanofiltration and separation membranes, monoliths for chromatographic techniques, size/shape-selective nanoreactors as well as catalytic supports.[1] Organic porous materials have unique properties over their inorganic nanostructured analogues, such as tunable mechanical properties, ease of functionalization, and lower production cost. The design of mesoporous polymeric materials with controlled morphology is not a trivial task.[2] In this context, the preparation of ordered nanoporous polymers through the selective degradation of one block from self-organized block copolymers has well been established by many groups.[3] In contrast, the use of (semi-)interpenetrating polymer networks (IPNs) as nanostructured precursors to (meso)porous polymer networks has been put forward only by a handful of research groups.[4,5]

IPNs represent an intimate association of two independently cross-linked polymers, at least one of which is synthesized in the immediate presence of the other.[6] Due to their peculiar interlocking framework, they have been the subject of widespread interest after it was discovered that they may develop microphase-separated co-continuous morphologies. It is noteworthy that if one of the sub-networks is degradable under specific conditions, and the other one is stable under identical conditions, (meso)-porous networks can be designed from such IPNs by resorting to selective degradation methods. In this regard, IPN systems based on a hydrolyzable polyester, such as poly

[1] Institut de Chimie et des Matériaux Paris-Est, CNRS – Université Paris XII, 2, rue Henri Dunant, 94320 Thiais, France
E-mail: grande@icmpe.cnrs.fr
[2] Laboratoire de Chimie de Provence, CNRS – Université de Provence, 13331 Marseille, France

(D,L-lactide) (PLA), and a vinylic polymer containing a non-hydrolyzable skeleton can be considered as appropriate precursors.

In continuation of recent systematic studies on the generation of (meso)porous polymer networks from PLA/poly(methyl methacrylate) (PMMA) (semi-)IPNs from one of us,[5] this report is concerned with the synthesis and characterization of functionalized porous frameworks engineered from miscellaneous functional (semi-)IPNs based on PLA and either methacrylic copolymers with acidic (COOH, SO_3H) functions or styrenic partners containing acidic (COOH, SO_3H) as well as basic (pyridine) functions.

Experimental Part

Materials

Dihydroxy-telechelic PLA (M_n (^{1}H NMR)= 1,700 g mol^{-1}; M_w/M_n (SEC) = 1.2) was synthesized by ring-opening polymerization of D,L-lactide initiated by the ethylene glycol/tin (II) octanoate system, as reported elsewhere.[7] 4,4',4''-triisocyanato-triphenylmethane (Desmodur® RU 1.25 mol L^{-1} in dichloromethane solution) was provided by Bayer. Dibutyltin dilaurate (DBTDL, Fluka) was used as received. Methyl methacrylate (MMA), methacrylic acid (Figure 1, MAA), styrene (S), 4-vinyl pyridine (Figure 1, 4 VP), and *para*-divinyl benzene (DVB) were purchased from Aldrich and distilled under vacuum prior to use. 4-vinylbenzoic acid (Figure 1, 4VBA, Alfa Aesar) and diurethane dimethacrylate (DUDMA, Aldrich) were used as received. Tetra-*n*-butyl ammonium 2-acrylamido 2-methyl propane 1-sulfonate (Figure 1, AMPS*) and tetra-*n*-butyl ammonium styrene 4-sulfonate (Figure 1, SS*) were prepared by classical ion-exchange reactions from 2-acrylamido 2-methyl propane 1-sulfonic acid (Fluka) and sodium styrene 4-sulfonate (Alfa Aesar), respectively. AIBN (Merck) was purified by recrystallization in methanol.

Preparation of Functional Semi-IPNs

PLA-containing methacrylic semi-IPNs were prepared by bulk free-radical copolymerization of MMA with DUDMA and/or MAA or AMPS*, initiated by AIBN, in the presence of PLA oligomer. The homogeneous initial mixture was introduced into a 2 mm-thick mould, heated to 65 °C for 2 h, and then cured at 110 °C for 2 h. Similarly, styrenic semi-IPNs were prepared by bulk free-radical copolymerization of S with DVB and/or 4VP or 4VBA or SS*, in the presence of the oligoester. In all instances, the initial AIBN concentration was kept constant at 2 mol % with respect to the total initial vinylic group concentration.

Extraction of PLA from Semi-IPNs

PLA-containing semi-IPNs were extracted for 24 h at 40 °C in a Soxhlet apparatus with dichloromethane (solvent reflux). The recovered sol fractions and extracted networks were dried under vacuum prior to further analyses. The amounts of sol fractions were calculated as the mass percentages of the extractables.

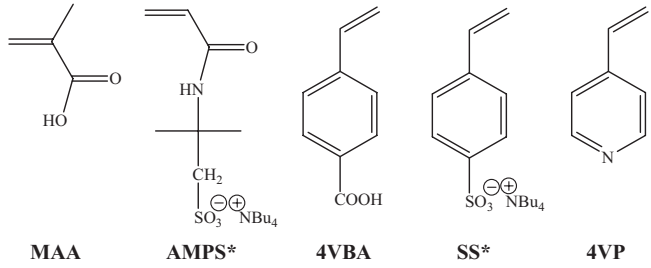

Figure 1.
Functional (meth)acrylic and styrenic monomers used for the synthesis of the corresponding semi-IPN and IPN systems.

Synthesis of Functional IPNs

IPNs composed of PLA and functional vinylic sub-networks were synthesized by the so-called *in-situ* sequential method,[8] following a procedure detailed in a previous report on PLA/PMMA-based systems.[5b]

Hydrolysis of PLA Sub-Network in IPNs

PLA-based IPNs were immersed in a mixture containing methanol and a 0.5 mol L^{-1} NaOH aqueous solution (H_2O/MeOH = 60/40 vol %) at 65 °C. After 48 h, the reaction medium was neutralized by a 0.1 mol L^{-1} HCl solution, and the residual networks were rinsed abundantly with distilled water up to neutral pH. For each network, the fractional mass loss (Δm) was assessed as follows: $\Delta m = (m_0 - m_d) / m_0$, where m_0 and m_d stand for the initial mass of the sample and its residual mass after vacuum drying, respectively.

Instrumentation

^{1}H NMR spectra were run using a Bruker AC 200 NMR spectrometer operating at a resonance frequency of 200 MHz. The size exclusion chromatography (SEC) equipment comprised a Spectra Physics P100 pump, two PL gel 5 μm mixed-C columns (Polymer Laboratories), and a Shodex RI 71 refractive index detector. The eluent was tetrahydrofuran (THF) at a flow rate of 1 mL min^{-1}; the calibration was performed using polystyrene (PS) standards. Fourier transform infra-red (FTIR) spectra were recorded between 4000 and 450 cm^{-1} on a Bruker Tensor 27 DTGS spectrophotometer in attenuated total reflection (ATR) mode. Glass transition temperature (T_g) and thermoporosimetry analyses were performed by differential scanning calorimetry (DSC) using a TA Instruments 2010 calorimeter. The scans were run from −50 to 250 °C for T_g analyses and from −50 to 5 °C for thermoporosimetry, at a heating rate of 20 and 1 °C min^{-1}, respectively.[5] Scanning electron microscopy (SEM) analyses were performed using a LEO 1530 microscope equipped with a high-vacuum (10^{-10} mm Hg) Gemini column. The accelerating tensions ranged from 1 to 5 kV. Prior to analyses, the samples were cryo-fractured and coated with a Pd/Au alloy (4 nm) in a Cressington 208 HR sputter-coater. The specific surface area values were quantified by nitrogen sorption porosimetry at 77 K using a Micromeritics ASAP 2010 gas adsorption instrument, and the data were exploited using the BET method in the relative pressure (P/P^0) range from 0.05 to 0.3.

Results and Discussion

Design of Functional Porous Networks from Semi-IPNs

Miscellaneous semi-IPN systems composed of uncross-linked PLA sub-chains entrapped in vinylic sub-networks bearing various functionalities were prepared by bulk free-radical copolymerization of monofunctional comonomers and a divinylic cross-linker, in the presence of PLA oligomers. The experimental conditions employed were identical to those previously used for similar systems, namely an AIBN-initiated cross-linking reaction at 65 °C for 2 h, followed by a 2 h curing process at 110 °C to ensure completion.[2,5a] The incorporation of all vinylic comonomers within the network structures was checked by FTIR through the total disappearance of the C=C stretching bands around 1640 cm^{-1}.

Functionalized porous polymer networks were readily generated by mere extraction of un-cross-linked PLA oligomers from the corresponding PLA-containing semi-IPNs (Figure 2). Such an extraction was effected using a good solvent for PLA at 40 °C, namely a temperature far below the T_g values of the methacrylic or the styrenic networks (*i.e.* 100-160 °C) to avoid the potential collapse of their resulting porous structures.[9] Regardless of the PLA composition, the nature, composition and cross-link density of the vinylic partner, the oligoester extraction was quantitative in all instances, as indicated by sol fractions close to the initial PLA compositions. The latter assertion was confirmed by the total disappearance of the characteristic bands of

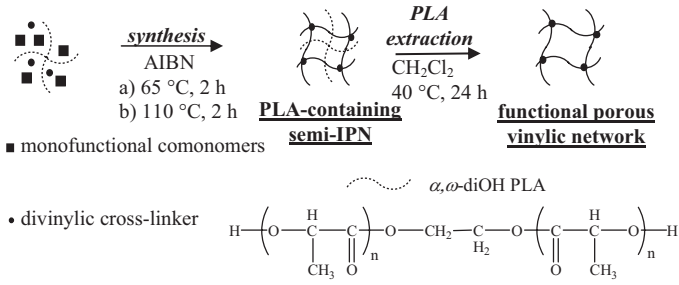

Figure 2.
Preparation of functional porous vinylic networks from semi-IPNs.

PLA (C=O and C–O stretching bands at 1745 and 1185 cm^{-1}, respectively) in the FTIR spectra of the residual networks. The COOH functionality was evidenced by FTIR with the presence of stretching bands due to free and hydrogen-bonded OH groups around 3550 and 2600 cm^{-1}, respectively.[10] In the case of $SO_3(H)$-functionalized networks, strong absorption bands were generally detected at 1260–1050 cm^{-1} and weak bands at 1050–1000 cm^{-1} due to the asymmetric and symmetric stretching of SO_3 groups.[10] The pyridine functionality was evidenced with the presence of the C=N stretching band around 1595 cm^{-1}.[10]

The morphology of semi-IPNs, before and after extraction, was examined using SEM. The non-extracted samples exhibited compact and non-porous structures. In sharp contrast, the micrographs of extracted semi-IPNs revealed highly porous structures with the pore sizes dependent on the structural parameters used (Figure 3a as an example, Tables 1 and 2).

We also determined pore sizes by thermoporosimetry through DSC measurements using water as the penetrant solvent. Thermoporosimetry is a quantitative and sensitive technique allowing for a reliable determination of pore size distributions in a wide array of (meso)porous materials, provided pore diameters are smaller than 200-300 nm.[11] As a matter of fact, from the melting thermograms of water contained in the porous networks, the melting temperature depression ($T_m - T_{m0}$) could be correlated to the pore diameter (D_p) as follows:[11] $D_p = 2.[0.68 - 32.33 / (T_m - T_{m0})]$, where T_m and T_{m0} are the melting temperatures of confined and bulk water, respectively. The pore diameter ranges thus obtained are listed in Tables 1 and 2; an example of pore size distribution is presented in Figure 3b. Overall, the results determined by SEM and DSC-based thermoporosimetry were in reasonable agreement to each other. Both analyses turned out to be complementary as SEM was more

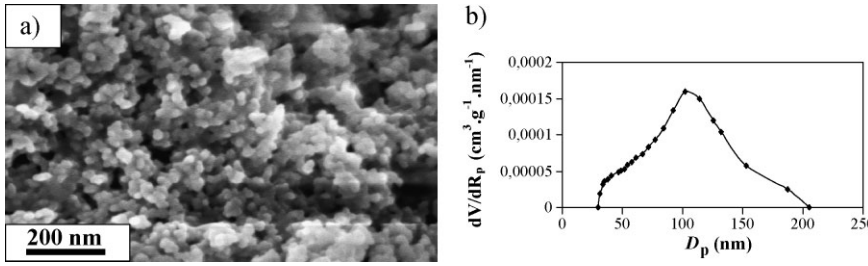

Figure 3.
(a) SEM micrograph of porous network derived from a methacrylic semi-IPN (see Table 1, entry **6** for characteristics), and (b) corresponding pore size distribution profile as determined by DSC-based thermoporosimetry.

Table 1.
Pore diameters of methacrylic porous networks derived from corresponding semi-IPNs as determined by SEM and DSC-based thermoporosimetry.

entry	methacrylic semi-IPN precursor	D_p (nm) SEM	D_p (nm) DSC
1	PLA/poly(MMA-*co*-MAA) 25/75 wt % (MMA/MAA = 50/50 mol %, 1 mol % DUDMA)	50 – 450	20 – 200[†]
2	PLA/poly(MMA-*co*-MAA) 50/50 wt % (MMA/MAA = 50/50 mol %, 1 mol % DUDMA)	75 – 475	50 – 300[†]
3	PLA/poly(MMA-*co*-MAA) 50/50 wt % (MMA/MAA = 50/50 mol %, 10 mol % DUDMA)	150 – 600	–
4	PLA/polyMAA 50/50 wt % (MMA/MAA = 0/100 mol %, 1 mol % DUDMA)	50 – 400	20 – 200[†]
5	PLA/poly(MMA-*co*-AMPS*) 25/75 wt % (MMA/AMPS* = 95/5 mol %, 1 mol % DUDMA)	40 – 175	20 – 150
6	PLA/poly(MMA-*co*-AMPS*) 50/50 wt % (MMA/AMPS* = 99/1 mol %, 1 mol % DUDMA)	25 – 200	30 – 200
7	PLA/poly(MMA-*co*-AMPS*) 50/50 wt % (MMA/AMPS* = 95/5 mol %, 1 mol % DUDMA)	15 – 200	20 – 180
8	PLA/poly(MMA-*co*-AMPS*) 50/50 wt % (MMA/AMPS* = 95/5 mol %, 5 mol % DUDMA)	50 – 250	20 – 200

[†]thermoporosimetry permitted determination of pore diameters up to 200-300 nm. For larger pore sizes, the melting peaks of "confined" and bulk water were not resolved: "confined" water behaved as a bulk solvent.

appropriate to characterize the larger pore sizes ($D_p > 200$ nm), while thermoporosimetry was more accurate to determine the smaller pore diameters ($D_p < 200$ nm).

Preliminary analyses by N_2 sorption porosimetry allowed for the determination of specific surface areas, thus providing values between 5 and 50 $m^2 g^{-1}$.

Table 2.
Pore diameters of styrenic porous networks derived from corresponding semi-IPNs as determined by SEM and DSC-based thermoporosimetry.

entry	styrenic semi-IPN precursor	D_p (nm) SEM	D_p (nm) DSC
9	PLA/poly(S-*co*-4VBA) 25/75 wt % (S/4VBA = 95/5 mol %, 1 mol % DVB)	10 – 210	15 – 200
10	PLA/poly(S-*co*-4VBA) 50/50 wt % (S/4VBA = 99/1 mol %, 1 mol % DVB)	10 – 290	30 – 300
11	PLA/poly(S-*co*-4VBA) 50/50 wt % (S/4VBA = 95/5 mol %, 1 mol % DVB)	10 – 300	15 – 200
12	PLA/poly(S-*co*-4VBA) 50/50 wt % (S/4VBA = 95/5 mol %, 5 mol % DVB)	10 – 350	15 – 270
13	PLA/poly(S-*co*-SS*) 25/75 wt % (MMA/SS* = 95/5 mol %, 1 mol % DVB)	25 – 65	20 – 70
14	PLA/poly(S-*co*-SS*) 50/50 wt % (MMA/SS* = 99/1 mol %, 1 mol % DVB)	20 – 140	20 – 100
15	PLA/poly(MMA-*co*-SS*) 50/50 wt % (MMA/SS* = 95/5 mol %, 1 mol % DVB)	30 – 100	25 – 70
16	PLA/poly(MMA-*co*-SS*) 50/50 wt % (MMA/SS* = 95/5 mol %, 5 mol % DVB)	30 – 120	30 – 80
17	PLA/poly(S-*co*-4VP) 25/75 wt % (S/4VP = 50/50 mol %, 1 mol % DVB)	50 – 125	20 – 150
18	PLA/poly(S-*co*-4VP) 50/50 wt % (S/4VP = 50/50 mol %, 1 mol % DVB)	50 – 250	20 – 250
19	PLA/poly(S-*co*-4VP) 50/50 wt % (S/4VP = 50/50 mol %, 10 mol % DVB)	70 – 500	20 – 200[†]
20	PLA/poly4VP 50/50 wt % (S/4VP = 0/100 mol %, 1 mol % DVB)	50 – 500	20 – 300[†]

[†]thermoporosimetry permitted determination of pore diameters up to 200-300 nm. For larger pore sizes, the melting peaks of "confined" and bulk water were not resolved: "confined" water behaved as a bulk solvent.

Design of Functional (Meso)Porous Networks from IPNs

Various IPNs constituted of PLA and methacrylic sub-networks were synthesized by the *in-situ* sequential method, *i.e.* by mixing all the precursors homogeneously, and then forming both networks *via* two successive and non-interfering cross-linking processes.[5b,8] Hence, the PLA sub-network was first generated at room temperature for 20 h from the dihydroxy-telechelic PLA oligomer through a DBTDL-catalyzed end-linking reaction with Desmodur® RU as a triisocyanate cross-linker. Subsequently, the methacrylic sub-network was created at 65 °C by AIBN-initiated copolymerization of MMA with DUDMA and/or MAA or AMPS* (2 h), and finally cured at 110 °C for 2 h (Figure 4). Styrenic IPNs were synthesized in a similar way using S and/or 4VP or 4VBA or SS* as vinylic comonomers and DVB as a cross-linker for the second sub-network formed. In all instances, the $[NCO]_0/[OH]_0$ and the $[DBTDL]_0/[PLA]_0$ initial ratios were equal to 1.4 and 0.44 respectively, in order to attain the higher conversion for the PLA sub-network formation.[5b]

All IPN samples were first subjected to a dichloromethane extraction for 24 h at 40 °C, and the values of sol fractions were lower than 10 wt %, indicating a near completion of the cross-linking processes. It is noteworthy that IPNs were transparent, before and after extraction, strongly suggesting good chain interpenetration of both constitutive sub-networks, and microdomain sizes smaller than about 150-200 nm, according to Okay.[12]

Advantage of the well-known hydrolytic degradability of PLA was taken to engineer functionalized (meso)porous networks with narrow pore size distributions through the hydrolysis of the PLA sub-network associated with partially hydrolyzable IPNs. As specified in Figure 4, this degradation was conducted at 65 °C using a mixture of a NaOH aqueous solution and methanol. The hydrolysis was performed at an intermediate temperature between the T_g of PLA sub-network (*i.e.* 20-45 °C) and those of vinylic sub-networks (*i.e.* around 100-160 °C) to avoid the collapse of the residual porous structures, while allowing for an efficient degradation of PLA.

All IPN samples and the corresponding single networks as model systems were subjected to hydrolysis under identical conditions. The PLA-based single network was completely degraded within 10 min. According to ^{1}H NMR and SEC analyses, the degradation products were composed of oligolactides, lactic acid, and cross-linker residues, indicating that the hydrolysis affected both ester and urethane functions. To understand how the conditions selected for PLA degradation might affect the structure of residual networks during the partial hydrolysis of IPNs, the corresponding single networks were analyzed after undergoing the same experimental conditions. Styrenic single networks remained unchanged, while slight mass losses ($\Delta m <$ 10 wt %) were assessed for methacrylic

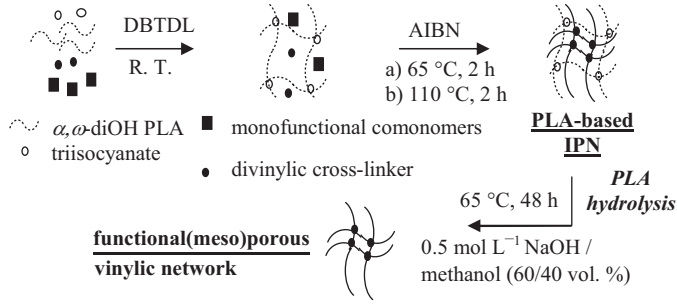

Figure 4.
Design of functional (meso)porous vinylic networks from IPNs.

Table 3.
Pore diameters of methacrylic porous networks derived from corresponding IPNs as determined by SEM and DSC-based thermoporosimetry.

entry	methacrylic IPN precursor	D_p (nm) SEM	D_p (nm) DSC
21	PLA/poly(MMA-*co*-MAA) 25/75 wt % (MMA/MAA = 50/50 mol %, 1 mol % DUDMA)	25 – 150	20 – 150
22	PLA/poly(MMA-*co*-MAA) 50/50 wt % (MMA/MAA = 50/50 mol %, 1 mol % DUDMA)	15 – 250	10 – 200
23	PLA/poly(MMA-*co*-MAA) 50/50 wt % (MMA/MAA = 50/50 mol %, 10 mol % DUDMA)	50 – 200	10 – 200
24	PLA/polyMAA 50/50 wt % (MMA/MAA = 0/100 mol %, 1 mol % DUDMA)	25 – 100	10 – 70
25	PLA/poly(MMA-*co*-AMPS*) 25/75 wt % (MMA/AMPS* = 95/5 mol %, 1 mol % DUDMA)	15 – 75	15 – 45
26	PLA/poly(MMA-*co*-AMPS*) 50/50 wt % (MMA/AMPS* = 99/1 mol %, 1 mol % DUDMA)	10 – 80	15 – 50
27	PLA/poly(MMA-*co*-AMPS*) 50/50 wt % (MMA/AMPS* = 95/5 mol %, 1 mol % DUDMA)	15 – 120	30 – 150
28	PLA/poly(MMA-*co*-AMPS*) 50/50 wt % (MMA/AMPS* = 95/5 mol %, 5 mol % DUDMA)	15 – 140	15 – 160

analogues. Mass loss decreased with increasing the concentration of the dimethacrylate cross-linker. As to IPN samples, mass loss values higher than or close to the initial compositions of PLA were reached after 48 h, indicating a quantitative degradation of the PLA sub-network. FTIR analyses of residual networks confirmed their pure vinylic structures through the total disappearance of the characteristic bands associated with the PLA component (N-$H_{urethane}$ and C=O stretching bands around 3370 and 1740 cm^{-1} respectively), while showing the presence of the desired functionalities.

Table 4.
Pore diameters of styrenic porous networks derived from corresponding IPNs as determined by SEM and DSC-based thermoporosimetry.

entry	styrenic IPN precursor	D_p (nm) SEM	D_p (nm) DSC
29	PLA/poly(S-*co*-4VBA) 25/75 wt % (S/4VBA = 95/5 mol %, 1 mol % DVB)	10 – 140	15 – 140
30	PLA/poly(S-*co*-4VBA) 50/50 wt % (S/4VBA = 95/5 mol %, 1 mol % DVB)	20 – 170	15 – 150
31	PLA/poly(S-*co*-4VBA) 50/50 wt % (S/4VBA = 90/10 mol %, 1 mol % DVB)	10 – 100	15 – 120
32	PLA/poly(S-*co*-4VBA) 50/50 wt % (S/4VBA = 95/5 mol %, 5 mol % DVB)	10 – 200	15 – 160
33	PLA/poly(S-*co*-SS*) 25/75 wt % (MMA/SS* = 95/5 mol %, 1 mol % DVB)	25 – 50	20 – 50
34	PLA/poly(S-*co*-SS*) 50/50 wt % (MMA/SS* = 99/1 mol %, 1 mol % DVB)	25 – 65	20 – 70
35	PLA/poly(MMA-*co*-SS*) 50/50 wt % (MMA/SS* = 95/5 mol %, 1 mol % DVB)	25 – 60	35 – 70
36	PLA/poly(MMA-*co*-SS*) 50/50 wt % (MMA/SS* = 95/5 mol %, 5 mol % DVB)	30 – 75	25 – 60
37	PLA/poly(S-*co*-4VP) 25/75 wt % (S/4VP = 50/50 mol %, 1 mol % DVB)	15 – 50	10 – 45
38	PLA/poly(S-*co*-4VP) 50/50 wt % (S/4VP = 50/50 mol %, 1 mol % DVB)	20 – 100	15 – 150
39	PLA/poly(S-*co*-4VP) 50/50 wt % (S/4VP = 50/50 mol %, 10 mol % DVB)	25 – 150	20 – 200
40	PLA/poly4VP 50/50 wt % (S/4VP = 0/100 mol %, 1 mol % DVB)	15 – 100	15 – 130

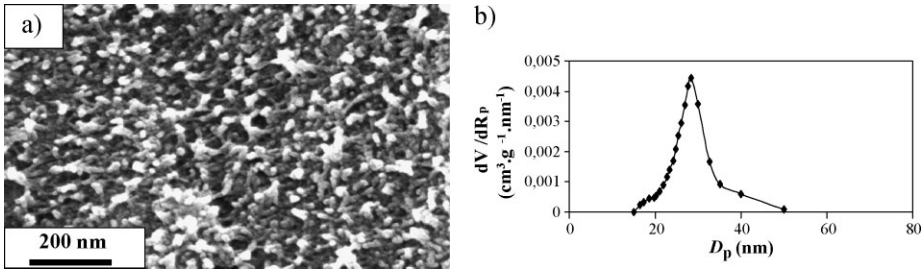

Figure 5.
(a) SEM micrograph of porous network derived from a methacrylic IPN (see Table 3, entry **26** for characteristics), and (b) corresponding pore size distribution profile as determined by DSC-based thermoporosimetry.

SEM and DSC-based thermoporometry analyses clearly showed that the functional vinylic networks resulting from PLA hydrolysis displayed porous structures with pore diameters smaller and pore size distributions narrower than those determined for their analogues derived from the corresponding semi-IPNs (Tables 3 and 4, Figure 5 as an example). Actually, the higher degree of chain interpenetration in IPN precursors may account for the decrease of pore sizes associated with residual networks and the narrowing of their pore size distributions. In IPN systems, the peculiar interlocking framework of both constituting sub-networks indeed restricts the spatial scale of phase separation to domains sizes of hundreds or even tens of nanometers, as inferred from the transparency of all samples. The IPN approach thus provides a valuable alternative for engineering mesoporous functional networks.

Furthermore, the specific surface areas were generally higher in IPN systems than in their semi-IPN analogues, in accordance with the occurrence of smaller pore sizes: values as high as $80\,m^2\,g^{-1}$ were thus obtained in preliminary analyses by N_2 sorption porosimetry.

Lastly, it is interesting to point out that the true density values of porous networks derived from IPN as well as semi-IPN systems – as determined by helium pycnometry at 25 °C – were very close to those of corresponding single networks (around 1.1-1.2). As the latter structures were compact and non-porous, such a match strongly suggested that the porous networks investigated were characterized by open pores or interconnected channels through which a fluid (gas or solvent) could flow. Furthermore, the pore volume (V_p) and the porosity ratio (P) values were evaluated through measurements of equilibrium mass swelling ratios in water. P values ranged from 0.2 to 0.5, depending on the PLA content in the precursors. Within experimental error, it can be assumed that such P values were in good agreement with those expected, especially taking into account the quantitative removal of the PLA partner from the semi-IPN or the IPN precursory networks.

Conclusion

This report broadens the spectrum of functionalized porous frameworks that can be engineered through the use of (semi-)IPNs as nanostructured precursors. The extraction of un-cross-linked PLA from semi-IPNs as well as PLA hydrolysis from partially hydrolyzable IPNs provide straightforward and effective routes to tune the porosity and functionality of porous three-dimensional scaffolds. Thus, PLA sub-chains, either un-cross-linked in semi-IPNs or cross-linked in IPNs, may effectively serve as porogen templates for the generation of such porous polymeric materials. The versatility of these complementary approaches has been illustrated through the generation of methacrylic porous networks

with acidic (COOH, SO_3H) functions as well as styrenic analogues with acidic (COOH, SO_3H) or basic (pyridine) functions by initially incorporating the corresponding functional vinylic monomers in the stable partners. Nevertheless, the systems considered need further investigation to precisely define the surface functionality of the pores.

The (meso)porous materials with controlled morphology and functionality tailored from functional (semi-)IPNs may find promising applications in separation techniques as chromatographic supports (functionalized stationary phases) and in the area of chemistry in confined media as nanoreactors.

Acknowledgements: Financial support of the National Agency for Research (programme ANR/PNANO, project POLYNANOCAT ''ANR-05-NANO-025'') is gratefully acknowledged.

[1] (a) G. Maier, *Angew. Chem. Int. Ed.* **1998**, *37*, 2960. (b) M. R. Buchmeiser, *Angew. Chem. Int. Ed.* **2001**, *40*, 3795. (c) H. P. Hentze, M. Antonietti, *Rev. Mol. Biotech.* **2002**, *90*, 27. (d) K. E. Rasmussen, S. Pedersen-Bjergaard, *Trends Anal. Chem.* **2004**, *23*, 1. (e) ''*Membrane Technology in the Chemical Industry*'', 2nd ed. S. Pereira-Nunes, K-. V. Peinemann, Eds., Wiley-VCH, Weinheim 2006.

[2] R. Balaji, S. Boileau, Ph. Guérin, D. Grande, *Polym. News* **2004**, *29*, 205.

[3] (a) J. S. Lee, A. Hirao, S. Nakahama, *Macromolecules* **1988**, *21*, 274. (b) T. Hashimoto, K. Tsutsumi, Y. Funaki, *Langmuir* **1997**, *13*, 6869. (c) J. L. Hedrick, K. R. Carter, R. Richter, R. D. Miller, T. P. Russell, V. Flores, D. Mecerreyes, Ph. Dubois, R. Jérôme, *Chem. Mater.* **1998**, *10*, 39. (d) G. J. Liu, J. F. Ding, T. Hashimoto, K. Kimishima, F. M. Winnik, S. Nigam, *Chem. Mater.* **1999**, *11*, 2233. (e) V. Z. H. Chan, J. Hoffman, V. Y. Lee, H. Iatrou, A. Avgeropoulos, N. Hadjichristidis, R. D. Miller, E. L. Thomas, *Science* **1999**, *286*, 1716. (f) T. Thurn-Albrecht, R. Steiner, J. DeRouchey, C. M. Stafford, E. Huang, M. Bal, M. Tuominen, C. J. Hawker, T. P. Russell, *Adv. Mater.* **2000**, *12*, 787. (g) D. A. Olson, L. Chen, M. A. Hillmyer, *Chem. Mater.* **2008**, *20*, 869.

[4] (a) J. M. Widmaier, L. H. Sperling, *Macromolecules* **1982**, *15*, 625. (b) F. Du Prez, E. J. Goethals, *Macromol. Chem. Phys.* **1995**, *196*, 903. (c) J. Hu, G. Pompe, U. Schulze, J. Pionteck, *Polym. Adv. Technol.* **1998**, *9*, 746. (d) N. Kayaman-Apohan, B. M. Baysal, *Macromol. Chem. Phys.* **2001**, 202. 1182.

[5] (a) G. Rohman, D. Grande, F. Lauprêtre, S. Boileau, Ph. Guérin, *Macromolecules* **2005**, *38*, 7274. (b) G. Rohman, F. Lauprêtre, S. Boileau, Ph. Guérin, D. Grande, *Polymer* **2007**, *48*, 7017.

[6] (a) L. H. Sperling, ''*Interpenetrating Polymer Networks and Related Materials*'', Plenum Press, New York 1981. (b) L. H. Sperling, V. Mishra, *Polym. Adv. Technol.* **1996**, *7*, *197*. (c) ''*IPNs Around the World: Science and Engineering*'', S. C. Kim, L. H. Sperling, Eds., Wiley, Chichester 1997.

[7] A. Bachari, G. Bélorgey, G. Hélary, G. Sauvet, *Macromol. Chem. Phys.* **1995**, *196*, 411.

[8] (a) H. Djomo, A. Morin, M. Damyanidu, G. C. Meyer, *Polymer* **1983**, *24*, 65. (b) S. R. Jin, G. C. Meyer, *Polymer* **1986**, *27*, 592. (c) S. R. Jin, J. M. Widmaier, G. C. Meyer, *Polymer* **1988**, *29*, 346.

[9] (a) D. Grande, J. L. Pastol, Ph. Guérin, S. Boileau, *Polym. Prepr. (Am. Chem. Soc., Div. Polym. Chem.)* **2003**, *44*(1), 44. (b) G. Da Costa, C. Gaillet, D. Grande, *Polym. Mater. Sci. Eng.* **2007**, *97*, 432.

[10] ''*Introduction to Infrared and Raman Spectroscopy*'', 3rd ed. N. B. Colthup, L. H. Daly, S. E. Wiberley, Eds., Academic Press, San Diego 1990.

[11] (a) M. Brun, A. Lallemand, J.-F. Quinson, C. Eyraud, *Thermochim. Acta* **1977**, *21*, 59. (b) J. N. Hay, P. R. Laity, *Polymer* **2000**, *41*, 6171. (c) J.-M. Nedelec, M. Baba, *Recent Res. Dev. Phys. Chem.* **2004**, *7*, 381.

[12] O. Okay, *Prog. Polym. Sci.* **2000**, *25*, 711.

